MOLECULAR PHARMACOLOGY, 22:554–564

Characterization of Nicotine Binding in Mouse Brain and Comparison with the Binding of α-Bungarotoxin and Quinuclidinyl Benzilate

MICHAEL J. MARKS AND ALLAN C. COLLINS[1]

Institute for Behavioral Genetics and School of Pharmacy, University of Colorado, Boulder, Colorado 80309

Received March 8, 1982; Accepted May 31, 1982

SUMMARY

The binding of [^{3}H]nicotine to mouse brain has been measured and subsequently compared with the binding of [^{125}I]α-bungarotoxin (α-BTX) and L-[^{3}H]quinuclidinyl benzilate (QNB). The binding of nicotine was saturable, reversible, and stereospecific. The average K_D and B_{max} were 59 nM and 88 fmoles/mg of protein, respectively. Although the rates of association and dissociation of nicotine were temperature-dependent, the incubation temperature had no effect on either K_D or B_{max}. When measured at 20° or 37°, nicotine appeared to bind to a single class of binding sites, but a second, very low-affinity, binding site was observed at 4°. Nicotine binding was unaffected by the addition of NaCl, KCl, $CaCl_2$, or $MgSO_4$ to the incubation medium. Nicotinic cholinergic agonists were potent inhibitors of nicotine binding; however, nicotinic antagonists were poor inhibitors. The regional distribution of binding was not uniform: midbrain and striatum contained the highest number of receptors, whereas cerebellum had the fewest. Differences in site densities, regional distribution, inhibitor potencies, and thermal denaturation indicated that nicotine binding was not the same as either QNB or α-BTX binding, and therefore that receptors for nicotine may represent a unique population of cholinergic receptors.

INTRODUCTION

The receptors for ACh[2] have been classified muscarinic and nicotinic primarily on the basis of interactions with various agonists and antagonists. The study of the muscarinic receptor (mAChR) has been facilitated by the development of specific ligands such as QNB (1); the nicotinic cholinergic receptor (nAChR) has been studied extensively with the elapid neurotoxin, α-BTX (2, 3). Although there appears to be general agreement that QNB binding provides a reliable estimate of the number of mAChR, the value of α-BTX for the study of the nAChR in mammalian brain has been questioned (4–8).

A wide variety of data suggests that α-BTX binding provides information relevant to cholinergic function in brain. The binding of α-BTX to brain is similar to binding to skeletal muscle and electroplaque ACh receptors. Apparent equilibrium dissociation constants for both muscle and electroplaque nAChR are very similar to that reported in brain (2). In addition, the regional distribution of α-BTX binding is very similar to that of choline acetyltransferase, the enzyme responsible for ACh synthesis (9), and the α-BTX binding component isolated from rat brain chromatographs in a pattern similar to that of the receptor isolated from the electroplaque (10). These observations indicate that α-BTX is an appropriate ligand for measuring brain nAChR. Despite these findings, the use of α-BTX to study the nAChR is controversial. The observations that α-BTX fails to inhibit neurotransmission in the autonomic ganglia of cat (4), chick (5), and rat (6) and in the spinal cord of frog (7) and cat (8) raise questions as to the physiological relevance of α-BTX binding detected in these tissues. Pharmacological studies of α-BTX binding have added to the controversy. Most notably, classical nicotinic antagonists such as decamethonium and hexamethonium are poor inhibitors of α-BTX binding to brain tissue (10–14).

These issues have led several groups to attempt to develop other means of measuring the nAChR in the mammalian central nervous system. Radiolabeled nicotine has been assessed as a potential ligand for brain nAChR (15–18). Some of these studies have lacked adequate controls for nonspecific binding (15), whereas in others a relatively inconvenient centrifugation procedure was used to separate bound and unbound ligand (16). Recently, Romano and Goldstein (17) reported the development of a convenient filtration assay which has

This work was supported in part by Grant CTR-1204 from the Council for Tobacco Research, U. S. A., Inc., and by Grant RR-07013-14, awarded by the Biomedical Research Support Grant Program, Division of Research Resources, National Institutes of Health.

[1] Recipient of National Institute on Alcohol Abuse and Alcoholism Research Scientist Development Award AA-00029.

[2] The abbreviations used are: ACh, acetylcholine; mAChR, muscarinic receptor; QNB, quinuclidinyl benzilate; nAChR, nicotinic cholinergic receptor; α-BTX, α-bungarotoxin; DFP, diisopropyl fluorophosphate; Hepes, 4-(2-hydroxyethyl)-1-piperazineethanesulfonic acid; DMPP, 1,1-dimethyl-4-phenylpiperazinium iodide.

0026-895X/82/060554-11$02.00/0

adequate controls for nonspecific binding. This study noted that nicotine binding was inhibited by micromolar concentrations of nicotinic agonists such as lobeline, carbamylcholine, and dimethylphenylpiperazinium. However, classical nicotinic antagonists such as decamethonium and *d*-tubocurarine had high IC_{50} values (near 0.1 mM). Other antagonists, such as hexamethonium, mecamylamine, and α-BTX, were virtually ineffective in blocking nicotine binding. These observations led Romano and Goldstein (17) to suggest that the long incubation used in their binding assays might have caused a shift in the cholinergic receptor to an agonist-selective state. Abood *et al.* (16), using a centrifugal assay method, also failed to detect potent inhibition of nicotine binding by nicotinic antagonists, including α-BTX, and suggested that the nicotine may be binding to noncholinergic sites in brain. Sershen *et al.* (18), using a filtration assay, reached a similar conclusion.

Thus, although the literature suggests that nicotine binds to neuronal tissue, the nature and significance of this binding is in question. Widely varying incubation conditions have been used to study nicotine binding. These differences include incubation time, incubation temperature, and buffer composition. The current report presents results of nicotine binding studies conducted at several temperatures, and provides a chromatographic identification of the bound radioactivity. In addition, nicotine, α-BTX, and QNB binding have been compared in several ways. These results indicate that all three ligands label cholinergic sites, but that these sites differ from one another.

EXPERIMENTAL PROCEDURES

Materials

Male DBA/2Ibg mice (60–90 days old) produced in the breeding colony of the Institute for Behavioral Genetics were used in the studies. The animals were housed in groups of two to five and were permitted free access to food and water. A 12-hr light/dark cycle (7 a.m.–7 p.m.) was maintained.

The radiolabeled compounds, DL-[^{3}H]nicotine (*N-methyl*-^{3}H, specific activity 61.2 Ci/mmole), [^{125}I]α-BTX (*Tyr*-^{125}I, specific activity 122 Ci/mmole), and L-[^{3}H] QNB (*benzylic*-4,4′-^{3}H, specific activity 40.2 Ci/mmole), were obtained from New England Nuclear Corporation (Newton, Mass.). [^{3}H]Nicotine was stored frozen in the presence of a 4-fold molar excess of mercaptoacetic acid (17).

The following compounds were obtained from Sigma Chemical Company (St. Louis, Mo.): bovine serum albumin, Tris, Tris hydrochloride, L-nicotine, L-lobeline hydrochloride, atropine sulfate, hexamethonium bromide, decamethonium bromide, *d*-tubocurarine chloride, tetraethylammonium bromide, gallamine triethiodide, mecamylamine hydrochloride, carbamylcholine chloride, carbamyl β-methylcholine chloride, L-polylysine (Type V), acetylcholine iodide, DFP, and Hepes. Oxotremorine and DMPP were purchased from Aldrich Chemical Company (Milwaukee, Wisc.). Ethyl acetate, tetramethylammonium bromide, and toluene were purchased from Baker Chemical Company (Phillipsburg, N. J.). Fisher Chemical Company (Fairlawn, N. J.) was the source of 2,5-diphenyloxazole, and Research Products International Corporation (Mount Prospect, Ill.) was the source of Triton X-100. Glass-fiber filters (GFC) were products of Whatman Ltd, and filmware scintillation bags were produced by Nalge Company (Rochester, N.Y.). α-BTX was purchased from Miami Serpentarium (Miami, Fla.). Gelman Instrument Company (Ann Arbor, Mich.) was the source of the ITLC SA chromatography sheets. The D-(+)-nicotine was a generous gift of Dr. Yukiteru Obi, of the Japan Tobacco and Salt Public Corporation (Yokohama, Japan).

Methods

Tissue preparation. Mice were killed by cervical dislocation and whole brains were removed, rinsed, and homogenized at 4° in 10 volumes of buffer (w/v) in a Dounce homogenizer. The buffer composition was as follows: NaCl, 118 mM; KCl, 4.8 mM; $CaCl_2$, 2.5 mM; $MgSO_4$, 1.2 mM; and Hepes, 20 mM; pH 7.5. The method of Romano and Goldstein (17) was used to prepare the crude membrane fraction. Briefly stated, the homogenate was centrifuged (20 min, 30,000 × *g*, 4°) and the resulting pellet was suspended in glass-distilled water (5%, w/v) and allowed to incubate for 1 hr at 4°. After this incubation, the suspension was centrifuged and the pellet was washed by rehomogenization in buffer, followed by centrifugation. This pellet was resuspended in buffer (15%, w/v) for use in the assays.

The brains were dissected into seven regions: cortex, cerebellum, hindbrain (pons-medulla), striatum, hippocampus, hypothalamus, and midbrain (including thalamus). Tissue preparation was identical with that used for whole brain. The small amounts of tissue available from a single mouse brain necessitated pooling regions from several (four to eight) animals.

[^{3}H]Nicotine binding. Nicotine binding routinely proceeded in a polypropylene test tube (12 mm × 75 mm), using 400–600 μg of protein in a final incubation volume of 250 μl. Binding was initiated by the addition of [^{3}H] nicotine to samples equilibrated to the final incubation temperature. At the completion of the incubation period (for equilibrium binding, incubation times were as follows: 4°, 2.5 hr; 20°, 15 min; and 37°, 5 min), the samples were diluted with 4 ml of ice-cold wash buffer (composition identical with that of incubation buffer, except that the Hepes concentration was reduced to 5 mM) and filtered under vacuum onto GFC filters which had been soaked in buffer containing 0.1% L-polylysine (17). The filters, containing the particulate protein and any bound nicotine, were subsequently washed four times with 4 ml of wash buffer. All filtrations and washes were conducted in a cold room (maintained at 4°), using buffers and filtration apparatuses cooled to 4°. This precaution was taken to minimize dissociation of the nicotine-receptor complex. Specific binding was determined as the difference in binding between samples containing 0 M and 1 × 10^{-5} M L-nicotine. Determinations were made in triplicate. Identical results were obtained with the use of 10^{-4} M L-lobeline, 10^{-4} M DMPP, 10^{-3} M carbamylcholine, or 10^{-3} M tetramethylammonium to establish blanks.

α-BTX binding. [^{125}I]α-BTX binding was conducted in a polypropylene test tube (12 mm × 75 mm) at 37°, using 200–300 μg of protein in a final incubation volume of 250

μl. Incubations were initiated by the addition of [^{125}I]α-BTX and lasted 2.5 hr (equilibrium reached at 1–2 hr). Filtration and wash were identical with those described for nicotine binding. The GFC filters were soaked in buffer containing 0.1% L-polylysine before use. Filtrations were carried out in the cold room. Blanks were determined in samples containing 1×10^{-6} M α-BTX.

[^{3}H]QNB binding. [^{3}H]QNB binding in whole brain was conducted at 37° using 20–30 μg of protein in a final incubation volume of 10 ml. For the regional analyses, the protein concentration was adjusted such that an average of 10% of the input counts were bound. Incubations were initiated by the addition of [^{3}H]QNB and lasted 45 min (equilibrium reached at 30 min). Upon completion of the incubation, samples were poured on the filters (L-polylysine treatment of filters is not required) and the tube was washed with 4 ml of buffer, after which the filters were washed twice more with 4 ml. While the wash buffer was maintained at 4°, it was not necessary to conduct the filtrations in the cold room. Blanks were determined in samples incubated with 1×10^{-6} M atropine.

Scintillation counting. After the samples were washed, the glass-fiber filters were placed in 10-ml Nalge filmware bags, and 2.5 ml of scintillation fluid (toluene, 1.35 liters; Triton X-100, 900 ml; 2,5-diphenyloxazole, 10.5 g) were added. After the bags were sealed, the filters were crushed and radioactivity was determined on a Beckman 7000 liquid scintillation spectrometer. Tritium was counted at 22% efficiency, and ^{125}I was counted at 80% efficiency.

Protein determination. Protein was determined using the method of Lowry *et al.* (19) with bovine serum albumin as standard. Determinations were made on 2-μl aliquots of the tissue suspension and with 2 μl of homogenization buffer used as the blank. With the low concentration of Hepes in the buffer and the small aliquot of sample assay, blanks showed less than 0.10 absorbance.

Time course determinations. The time course for nicotine binding was determined as described above, except that samples were filtered and washed after several different incubation times. For binding at 4°, these times were 5–180 min; at 20°, 30 sec–20 min; at 37°, 10 sec–10 min. Triplicate samples were collected at each time point for both total binding (0 M L-nicotine) and blanks (1×10^{-5} M L-nicotine).

The time course for nicotine dissociation was studied by using tissue which had been incubated with [^{3}H]nicotine for 2.5 hr at 4°. The incubation volume of 2.5 ml contained 4–6 mg of particulate protein (the concentration of protein was the same as that used in standard binding assays). The concentration of [^{3}H]nicotine used in these experiments was 31.5 ± 3.1 mM (mean ± SEM). After the 2.5-hr incubation at 4°, 0.25 ml of suspension was removed, filtered, and washed to determine binding at zero dissociation time. The samples were then diluted 10-fold with buffer at 4°, 20°, or 37°. The dilution buffer contained 1×10^{-5} M L-nicotine. At specified times after dilution, 2.5-ml aliquots of the diluted samples were removed, filtered, and washed. The amount of specifically bound nicotine remaining at each time was determined from the difference in radioactivity present between samples in which binding was achieved with 0 M L-nicotine present and samples in which binding was achieved with 1×10^{-5} M L-nicotine present.

Nicotine binding as a function of protein. The dependence of [^{3}H]nicotine binding on the protein present in the incubation medium was determined by using the standard assay at 37°. The protein content of the incubations was varied between 0 μg and 1150 μg.

Saturability of binding. Saturability of nicotine binding was studied by varying the concentration of DL-[^{3}H]nicotine between 10 nM and 200 nM. Specific binding was calculated as the difference in binding obtained with 0 M and 1×10^{-5} M L-nicotine present. The saturability of [^{125}I]α-BTX and [^{3}H]QNB binding was studied by varying the amount of added radiolabeled ligand. The blanks for these experiments were 1×10^{-6} M α-BTX and 1×10^{-6} M atropine, respectively. All K_D and B_{max} values were calculated by linear regression analysis of Scatchard plots of the data.

Thermal sensitivity of binding. The effect of prior incubation at elevated temperatures on ligand binding was investigated by incubating whole brain particulate fractions (protein concentration 12 mg/ml) for various times at temperatures of 58°, 63°, 68°, 73°, and 78°. Incubations were initiated by the addition of 2 ml of membrane suspension (50 mg/ml) to 6 ml of buffer warmed to the final incubation temperature. At several times after this addition (from 1 min to 30 min), the samples were mixed, and 1-ml aliquots of the suspension were removed and placed in test tubes cooled in an ice bath. These aliquots were then used to determine binding at 37°, using the standard binding assays. The decay constants were determined at each temperature by linear regression analysis of the plot of log(%activity remaining) versus time for each ligand.

Identification of bound radioactivity. [^{3}H]Nicotine was bound to whole brain particulate fraction in the presence or absence of 1×10^{-5} M L-nicotine. Twelve filters from each incubation were combined, and 5 nmoles of L-nicotine were added as carrier. The filters were crushed in 3 ml of 0.1 M NaOH and 5 ml of ethyl acetate. The supernatant was collected by filtration and extracted with shaking for 15 min. After centrifugation, the ethyl acetate layer was collected. The filters were crushed twice more with ethyl acetate, which was collected by filtration and shaken with the 0.1 M NaOH. The ethyl acetate extracts were combined and shaken with 1 ml of 0.1 M HCl. After centrifugation, the ethyl acetate was discarded, the 0.1 M HCl was neutralized with 1 M NaOH, and the solution was made basic (pH 12) with the addition of more 1 M NaOH. This aqueous solution was extracted three times with 3-ml aliquots of ethyl acetate. The ethyl acetate extracts were combined and evaporated to dryness under a stream of nitrogen gas. Absolute methanol (200 μl) was added to both tubes, and 50 μl of methanol solution were spotted on ITLC-SA chromatography sheets. The sheets were developed in either of two solvent systems: (a) $CHCl_3$, 82; C_2H_5OH, 25; NH_4OH, 0.25; or (b) CH_3OH, 99; NH_4OH, 1. Authentic L-nicotine was applied to the sheets, as well. After the chromatograms were developed, spots were visualized by exposure to iodine vapors. The chromatography sheets were then

cut into 1-cm strips and radioactivity was determined. This extraction procedure provides a recovery of greater than 90% of the counts added to samples treated in parallel. Extraction into 0.1 N HCl and then back-extraction from the alkalinized 0.1 N HCl solution were required to reduce the lipid content of the samples.

RESULTS

Characterization of Nicotine Binding

Time course of nicotine binding and dissociation. The time courses for [^{3}H]nicotine binding to whole brain particulate protein at 4°, 20°, and 37° are shown in Fig. 1. Equilibrium was attained after 2 min at 37°, 5 min at 20°, and approximately 1 hr at 4°. Although the time required to reach equilibrium at these temperatures differed greatly, no differences in equilibrium binding were observed.

The effect of temperature on the dissociation of bound [^{3}H]nicotine is shown in Fig. 2. The rate of dissociation was also markedly affected by temperature. The rate constant for this process increased from 0.0155 ± 0.0023 min^{-1} at 4°, to 0.280 ± 0.048 min^{-1} at 20°, to 1.511 ± 0.140 min^{-1} at 37° (mean ± SD). These constants correspond to half-lives for binding of 44.8 ± 4.8 min at 4°, 2.5 ± 0.6 min at 20°, and 0.46 ± 0.08 min at 37° (mean ± SD). The linearity of the curves at each temperature suggests that a single process, with a considerable temperature coefficient, occurred. The experiments also demonstrate the reversibility of nicotine binding.

Protein dependence of DL-[^{3}H]nicotine binding. The effect of altering the amount of protein present in the incubation medium on [^{3}H]nicotine binding is shown in Fig. 3. Nonspecific binding of [^{3}H]nicotine (that occurring in the presence of 1×10^{-5} M L-nicotine) increased linearly with protein; however, total binding displayed some curvature at higher protein concentrations. Specific binding, obtained by subtracting the binding occurring in the presence of 1×10^{-5} M L-nicotine from that occurring in the absence of L-nicotine, was linear with protein to 800 μg. All subsequent determinations on [^{3}H]nicotine binding were conducted with less than 800 μg of protein present in the assay.

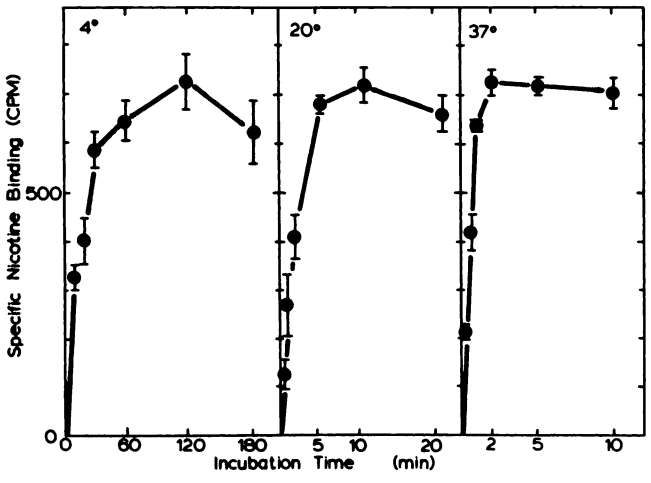

FIG. 1. *Time course of nicotine binding as a function of temperature*

Whole brain particulate protein was incubated with DL-[^{3}H]nicotine (36.4 nM) at the temperatures indicated. At the times shown, three control samples (L-nicotine = 0 M) and three blank samples (L-nicotine = 10^{-5} M) were filtered and washed. Each point represents the mean ± standard error of the mean of specifically bound counts.

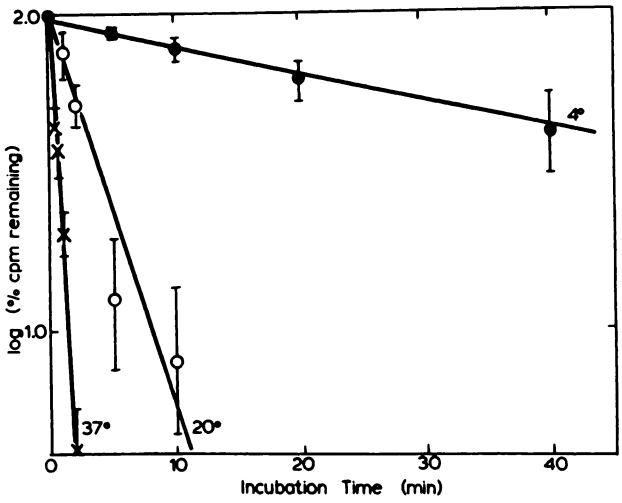

FIG. 2. *Effect of incubation temperature on nicotine dissociation*

The dissociation of [^{3}H]nicotine from whole-mouse brain particulate fraction was determined after dilution of samples, to which nicotine had been bound, with buffer containing unlabeled L-nicotine. Dissociation of specifically bound counts was determined by comparison of samples in which [^{3}H]nicotine binding was achieved in the presence or absence of 10^{-5} M L-nicotine. Each point represents the mean ± standard error of the mean determined from three experiments at each temperature.

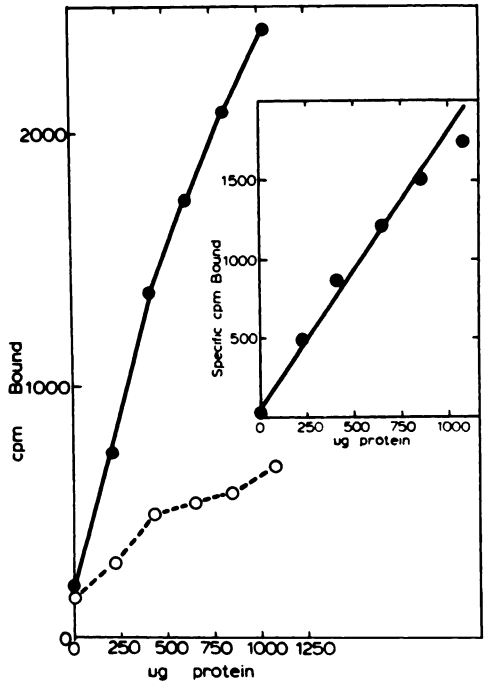

FIG. 3. *Protein dependence of nicotine binding*

DL-[^{3}H]Nicotine (36.4 nM) was incubated for 5 min at 37° with varying amounts of particulate protein. Binding in the presence of 0 M L-nicotine (●) or 1×10^{-5} M L-nicotine (○) was measured. The *inset* shows the difference in binding between those samples containing 0 M or 10^{-5} M L-nicotine.

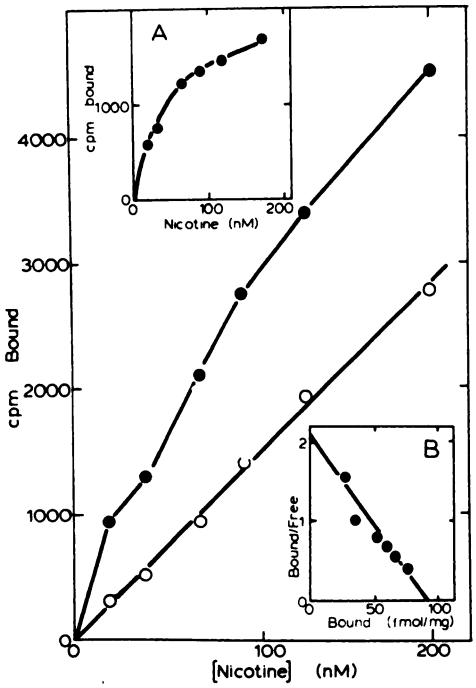

FIG. 4. *Saturability of [^{3}H]nicotine binding*

Brain particulate protein was incubated for 5 min at 37° with varying amounts of [^{3}H]nicotine in the presence (○) or absence (●) of 1×10^{-5} M L-nicotine. *Inset A* shows the difference in binding between samples containing 0 M and 10^{-5} M L-nicotine; *inset B* presents the data of *inset A* as a Scatchard plot.

Saturability of nicotine binding. The effect of changing [^{3}H]nicotine concentration on ligand binding is shown in Fig. 4. Nonspecific binding increased linearly with added [^{3}H]nicotine. Total binding showed modest curvature as drug concentration was raised. A plot of specific binding (*inset A*) appeared to form a rectangular hyperbola. Representation of these data as a Scatchard plot (*inset B*) generated a straight line, a result consistent with that expected from a single nicotine binding site. The apparent K_D determined in this experiment was 44 nM and the B_{max} was 94 fmoles/mg of protein. The Hill coefficient of 1.02 ± 0.06, which was obtained from data gathered in three separate experiments, further indicates that neither positive or negative cooperativity nor multiple nicotine binding sites are likely. Identical K_D and B_{max} values were obtained by using 10^{-5} M L-nicotine, 10^{-4} M L-lobeline, 10^{-4} M DMPP, 10^{-3} M carbamylcholine, or 10^{-3} M tetramethylammonium to establish blank values.

Effect of temperature on DL-[^{3}H]nicotine binding. The inhibition of [^{3}H]nicotine binding by L-nicotine at 4° and 37° is shown in Fig. 5. Although the log dose-response curve for inhibition at 37° fits a one-site model (IC_{50} = 3.5×10^{-8} M), that obtained at 4° is more complex. The inhibition observed at 4° seems to fit a two-site model. The components of the model were estimated by using a least-squares method involving successive approximations. One site, with an IC_{50} of 2.5×10^{-8} M, represents 72% of the [^{3}H]nicotine sites; the second site, with an IC_{50} of 5×10^{-5} M, represents the remaining 28% of the sites. The amount of [^{3}H]nicotine binding inhibited by low L-nicotine concentrations at 4° (23.5 ± 1.1 fmoles/mg of protein, [^{3}H]nicotine concentration = 27.5 ± 2.2 nM, n = 3) was equal to total L-nicotine-inhibitable [^{3}H]nicotine binding at 37° (24.4 ± 2.4 fmoles/mg of protein, [^{3}H]nicotine concentration = 26.2 ± 3.6 nM, n = 4). The site inhibited by high concentrations of nicotine at 4° had very low affinity for [^{3}H]nicotine and was found only at low temperatures. The binding of [^{3}H]nicotine was also inhibited by D-nicotine at both 4° and 37°. The IC_{50} value for D-nicotine inhibition at 37° was 1.2 μM, a value which is approximately 30-fold greater than the IC_{50} for L-nicotine. Likewise, the IC_{50} for inhibition of [^{3}H]nicotine binding at 4° was 1 μM at the high-affinity site. Although L-nicotine was 40-fold more potent as an inhib-

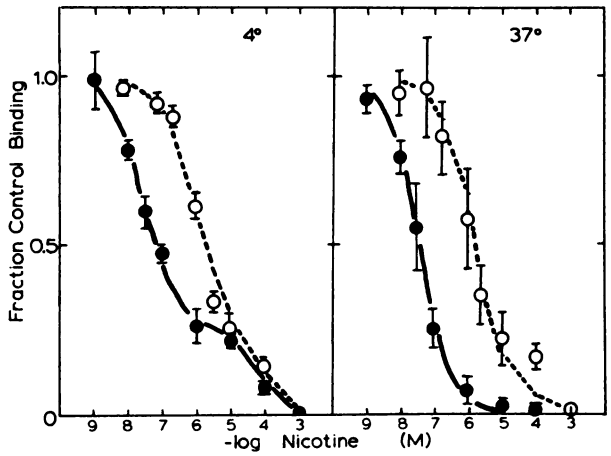

FIG. 5. *Effect of temperature on nicotine inhibition of DL-[^{3}H]nicotine binding*

Whole-brain particulate fraction was incubated for 2.5 hr at 4° or for 5 min at 37° with [^{3}H]nicotine (30.6 ± 1.0 nM) and the indicated concentrations of L-nicotine (●) or D-nicotine (○). Each point represents the mean ± standard error of the mean determined from three separate experiments. Binding occurring at 1×10^{-3} M L-nicotine was used as the blank.

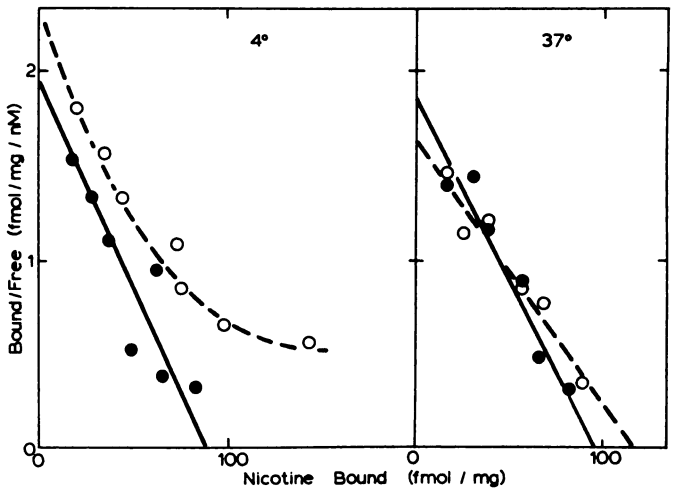

FIG. 6. *Effect of incubation temperature and L-nicotine concentration on Scatchard plots for DL-[^{3}H]nicotine binding*

Whole-brain particulate fraction was incubated at 4° for 2.5 hr or at 37° for 5 min. Specific nicotine binding was subsequently calculated using the counts bound in the presence of 1×10^{-5} M (●) or 1×10^{-3} M (○) L-nicotine as the blanks.

itor of [^{3}H]nicotine at the high-affinity site, no difference between the isomers was detected at the low-affinity site.

The biphasic inhibition of [^{3}H]nicotine binding by L-nicotine at 4° should also result in nonlinear Scatchard plots when 1×10^{-3} M L-nicotine is employed as the blank. Therefore, Scatchard plots of [^{3}H]nicotine binding at 4° and 37° were constructed using either 1×10^{-5} M or 1×10^{-3} M L-nicotine to establish blank values. These results are presented in Fig. 6. The use of either 10^{-5} M or 10^{-3} M L-nicotine to determine nonspecific binding had no effect on the Scatchard plots of [^{3}H]nicotine binding at 37°. The K_D (48.6 nM with 10^{-5} M and 67.4 nM with 10^{-3} M) and B_{max} (94 fmoles/mg with 10^{-5} M and 114 fmoles/mg with 10^{-3} M) are not significantly different. The plots showed no sign of curvature. However, when incubation was conducted at 4°, different results were obtained. When blank values were determined by using 1×10^{-5} M nicotine, the Scatchard plot was linear and its K_D and B_{max} (39 nM and 82 fmoles/mg, respectively) were comparable to those values obtained at 37°. However, the use of 10^{-3} M L-nicotine to determine blank values generated a distinctly nonlinear Scatchard plot, which may be interpreted to represent multiple binding sites, negative cooperativity, or an inaccurate definition of specific binding (20).

It should be noted that the Scatchard plots obtained at 20° were similar to those observed at 37° (data not shown). The K_D values obtained using 1×10^{-5} M and 1×10^{-3} M nicotine as blanks were 47.1 nM and 62.6 nM, and the B_{max} values were 100 pmoles/mg and 105 pmoles/mg, respectively. These values are comparable to those obtained at 37° and at 4° using 1×10^{-5} M nicotine as the blank.

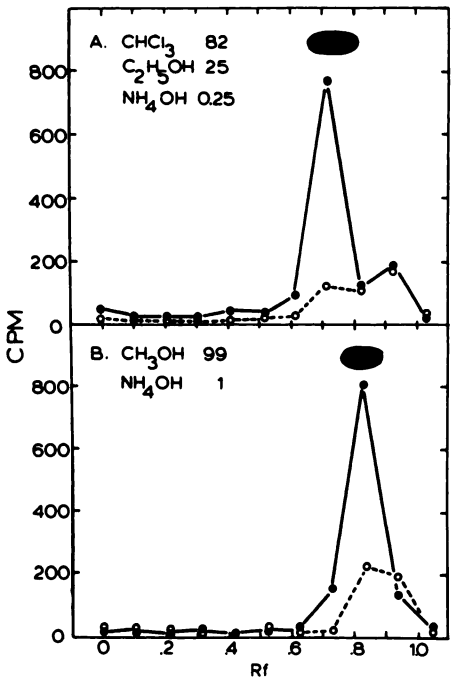

FIG. 7. *Chromatographic identification of bound radioactivity*

DL-[^{3}H]Nicotine bound in the presence (○) or absence (●) of 1×10^{-5} M L-nicotine was extracted and chromatographed. The counts present in each region of the chromatograms, developed in two solvent systems (A and B), are shown. The *dark ovals* represent the area stained by iodine vapors after chromatography of authentic L-nicotine.

TABLE 1

Binding of nicotine, α-BTX, and QNB in whole brain

K_D and B_{max} were determined from Scatchard plots in three to five separate experiments. Means ± standard error of the mean of the data are shown.

Ligand	K_D	B_{max}
	nM	*fmoles/mg*
Nicotine	58.6 ± 15.0	88.2 ± 6.7
α-BTX	0.12 ± 0.04	22.7 ± 1.8
QNB	0.037 ± 0.005	1959 ± 124

The identity of the binding characteristics obtained from Scatchard analysis is consistent with the observation that equilibrium binding (blank = 1×10^{-5} M L-nicotine) is independent of incubation temperature (Fig. 1). The constancy of the K_D for [^{3}H]nicotine binding as a function of temperature indicates that the association rate constant and dissociation rate constant are affected equally by temperatures between 4° and 37°.

The inhibition of high-affinity [^{3}H]nicotine binding at 4° by a number of nicotinic agonists was also determined. The K_I values obtained were as follows: DMPP, 0.2 μM; carbamylcholine, 2 μM; and tetramethylammonium, 7 μM. These values are nearly identical with those obtained at 37° (Table 3). Total binding at the high-affinity site at 4° and total binding at 37° were equal. This finding, and the similarity in K_D for DL-[^{3}H]nicotine binding, as well as the similar potencies of D- and L-nicotine in inhibiting [^{3}H]nicotine binding and the identity of K_I values for the inhibition of binding by nicotinic agonists, argue that the high-affinity site measured at 4° is the same as the single binding site seen at 37°.

Cation effects. The addition of up to 200 mM NaCl, 20 mM KCl, 10 mM $MgSO_4$, or 10 mM $CaCl_2$ to cation-free Hepes buffer had no significant effect on nicotine binding measured at 37°.

Effect of boiling. Boiling of tissue for 5 min completely abolished specific nicotine binding, but resulted in a 25% increase in nonspecific binding measured at 37°.

Identification of bound radioactivity. The radioactivity bound to whole-brain particulate protein was extracted and chromatographed as described under Methods. The results are shown in Fig. 7. Although a significant portion of the nonspecifically bound counts does not migrate with authentic L-nicotine in either solvent system tested, the specifically bound counts comigrate with nicotine. It seems likely that the specifically bound radioactivity is, indeed, [^{3}H]nicotine.

Comparison of Nicotine Binding with That of Other Cholinergic Ligands

Whole-brain binding properties. The K_D and B_{max} for [^{3}H]nicotine, [^{125}I]α-BTX, and [^{3}H]QNB were determined by Scatchard analysis in the whole-brain particulate fraction. The results are summarized in Table 1. There are more than 20 times as many [^{3}H]QNB binding sites in whole brain as there are [^{3}H]nicotine sites. Nicotine sites exceed [^{125}I]α-BTX sites by about 4-fold.

Regional distribution of ligand binding. The distri-

bution of [^{3}H]nicotine, [^{125}I]α-BTX, and [^{3}H]QNB binding sites was determined in seven mouse brain regions and in whole brain. These results are given in Table 2. A single concentration of each ligand was used in these determinations. [^{3}H]Nicotine binding was greatest in the midbrain region and somewhat lower in striatum. Both of these regions had a greater density of [^{3}H]nicotine binding sites than did whole brain. Cortex, hindbrain, and hypothalamus showed very similar levels of nicotine binding, and this binding was slightly less than that in whole brain, whereas hippocampal nicotine binding was about 70% of that found in whole brain. The cerebellum had the fewest number of sites. The regional distribution of [^{125}I]α-BTX binding sites was somewhat different from that of [^{3}H]nicotine binding sites. Hindbrain, hippocampus, and hypothalamus had densities of [^{125}I]α-BTX sites higher than the density in whole brain, but the greatest concentration of binding sites was found in the striatum. Cortex and midbrain possessed slightly fewer [^{125}I]α-BTX sites than did whole brain, whereas cerebellum had the lowest density of these sites. Regional distribution of [^{3}H]QNB sites indicated that the density of drug binding in cortex and hippocampus was greater than that in whole brain, and that the striatum had the greatest density of sites. Hindbrain, midbrain, and hypothalamus had considerably fewer QNB binding sites than did whole brain, and cerebellum had the fewest number of sites.

In order to compare the regional distribution quantitatively, binding in each region was calculated as a fraction of whole-brain binding. Analysis of regional binding in this way reveals several differences in distribution among the three ligands. The ratios between nicotine and α-BTX binding differ significantly in midbrain, hippocampus, and hypothalamus, with a larger ratio for nicotine in midbrain and a larger ratio for α-BTX in the other two regions. Nicotine and QNB ratios differ in every region but striatum: the nicotine ratio is greater in cerebellum, midbrain, hindbrain, and hypothalamus, and the QNB ratio is greater in cortex and hippocampus. QNB and α-BTX binding have differing ratios in cortex, hindbrain, and hypothalamus; the ratios for α-BTX are greater in the latter two regions. These results demonstrate that the regional distribution of nicotine binding does not directly parallel that of either α-BTX or QNB, nor do α-BTX and QNB binding directly parallel each other.

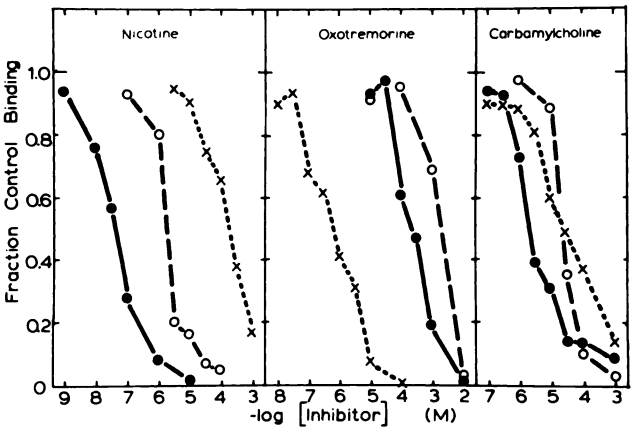

FIG. 8. *Effect of inhibitors on [^{3}H]nicotine, [^{125}I]α-BTX, and [^{3}H]QNB binding*

Nicotine (●, 29.9 nM), α-BTX (○, 0.37 nM), and QNB (×, 43.4 pM) were each incubated with varying concentrations of L-nicotine, oxotremorine, or carbamylcholine as indicated. All incubations were performed at 37°. Data are presented as fractions of control binding and represent the results of four experiments. The blank values were determined by using 1×10^{-5} M L-nicotine for nicotine, 1×10^{-6} M unlabeled α-BTX for α-BTX, and 1×10^{-6} M atropine for QNB.

Inhibition of ligand binding by cholinergic agents. The effect of nicotinic and muscarinic agonists and antagonists on the binding of [^{3}H]nicotine, [^{125}I]α-BTX, and [^{3}H]QNB was examined to provide a further comparison of these sites. The log dose-response curves for inhibition of the binding of the three ligands by nicotine, oxotremorine, and carbamylcholine are shown in Fig. 8. The nicotinic agonist, L-nicotine, was most effective in inhibiting the binding of [^{3}H]nicotine; it also inhibited the binding of [^{125}I]α-BTX at low concentrations. The inhibition by L-nicotine of [^{3}H]QNB binding occurred at much higher concentrations. On the other hand, oxo-

TABLE 2

Regional distribution of nicotine, α-BTX, and QNB binding

Binding (femtomoles per milligram of protein) was determined as described under Methods. The blanks were 1×10^{-5} M nicotine, 1×10^{-6} M α-BTX, and 1×10^{-6} M atropine for nicotine, α-BTX, and QNB binding, respectively. The concentrations of radiolabeled ligands were as follows: 32.3 ± 0.8 nM (0.57 K_D) for nicotine, 0.35 ± 0.07 nM (2.9 K_D) for α-BTX, and 33.0 ± 5.3 pM (0.90 K_D) for QNB. Means ± standard error of the mean for drug binding, and ratios between regional binding and that in whole brain, were determined in four separate experiments. Ratios were compared within a region by one-way analysis of variance followed by Tukey's (*b*) *post hoc* test.

Brain region	Nicotine		α-BTX		QNB	
	Bound	Ratio	Bound	Ratio	Bound	Ratio
Whole brain	28.8 ± 2.1	—	16.1 ± 1.2	—	974 ± 100	—
Cortex	23.5 ± 2.8	0.81 ± 0.06	14.2 ± 0.9	0.86 ± 0.02	1187 ± 107	1.23 ± 0.03[a, b]
Cerebellum	7.9 ± 0.9	0.28 ± 0.04	3.6 ± 0.1	0.22 ± 0.01	126 ± 18	0.14 ± 0.03[a]
Hindbrain	24.7 ± 3.6	0.84 ± 0.09	17.6 ± 1.9	1.08 ± 0.08	453 ± 16	0.48 ± 0.03[a, b]
Midbrain	48.7 ± 8.0	1.67 ± 0.20	15.3 ± 1.0	0.96 ± 0.08[a]	584 ± 46	0.61 ± 0.04[a]
Hippocampus	20.7 ± 3.7	0.69 ± 0.09	17.6 ± 1.4	1.08 ± 0.12[a]	1032 ± 48	1.08 ± 0.07[a]
Hypothalamus	24.9 ± 2.9	0.87 ± 0.12	20.5 ± 2.6	1.23 ± 0.10[a]	502 ± 62	0.52 ± 0.03[a, b]
Striatum	38.3 ± 5.6	1.30 ± 0.11	23.1 ± 1.5	1.41 ± 0.10	1523 ± 125	1.70 ± 0.17

[a] Ratios were significantly different from those obtained for nicotine binding ($p < 0.05$).

[b] Regional ratios for QNB binding were significantly different from those for α-BTX binding ($p < 0.05$).

tremorine, a muscarinic agonist, is a potent inhibitor of [^{3}H]QNB binding. It inhibited [^{3}H]nicotine and [^{125}I]α-BTX binding at much higher concentrations, but with very similar IC_{50} values for these two ligands. Inhibition of the binding of the three ligands by carbamylcholine, a general cholinergic agonist, occurred at very similar concentrations of this agonist.

The effect of several other compounds on the binding of [^{3}H]nicotine, [^{125}I]α-BTX, and [^{3}H]QNB was determined. The results are summarized in Table 3. The nicotinic agonists L-nicotine, L-lobeline, tetramethylammonium, DMPP, and carbamylcholine effectively inhibited nicotine binding (apparent K_I of 3 μM or less). These compounds were also effective in blocking [^{125}I]α-BTX binding, but, with the exception of tetramethylammonium, the K_I values were higher than those for nicotine. The compounds that showed the greatest difference between [^{3}H]nicotine and [^{125}I]α-BTX were L-nicotine and L-lobeline. With the exception of the effect of L-lobeline on α-BTX binding, nicotinic agonists were less potent inhibitors of [^{3}H]QNB binding than they were of either [^{3}H]nicotine or [^{125}I]α-BTX binding. As shown in Fig. 8 and in Table 3, carbamylcholine is nearly equipotent in its inhibition of the binding of all three ligands. In addition, the effect of acetylcholine on nicotine binding was determined in tissue which had been incubated twice for 5 min with DFP (10 μg/ml). This treatment completely (>99.9%) inhibited acetylcholinesterase. Acetylcholine was a potent inhibitor of [^{3}H]nicotine binding. The K_I for acetylcholine, 0.4 μM, was one-fifth that for its nonhydrolyzable analogue, carbamylcholine. The muscarinic agonists, β-methylcarbamylcholine and oxotremorine, and the muscarinic antagonist, atropine, were much more effective in inhibiting [^{3}H]QNB binding than in inhibiting nicotine or α-BTX binding. With the exception of the inhibition of [^{125}I]α-BTX by nonradioactive α-BTX, nicotinic antagonists were poor inhibitors of all three ligands and showed little or no selectivity in their inhibition. A high concentration of α-BTX had no effect on either [^{3}H]nicotine or [^{3}H]QNB binding.

TABLE 3

Inhibition of nicotine, α-BTX, and QNB binding

Apparent K_I values were calculated from log dose-response curves for inhibition of ligand binding. Average [^{3}H]nicotine concentration was 29.9 nM (0.52 K_D), average [^{125}I]α-BTX concentration was 0.37 nM (3.08 K_D), and average [^{3}H]QNB concentration was 43.4 pM (1.17 K_D). Values represent means ± standard error of the mean of K_I values calculated from IC_{50} values for three individual experiments using the method of Cheng and Prusoff (21). Because of the slow binding of α-BTX, tissue was incubated with nonradioactive α-BTX for 2 hr before the addition of either nicotine or QNB. This incubation had no effect on the control binding of either ligand. All K_I values are given in micromolar concentrations.

Inhibitor	Nicotine	α-BTX	QNB
L-Nicotine	0.023 ± 0.008	0.81 ± 0.22	94 ± 33
L-Lobeline	0.15 ± 0.04	8.6 ± 0.1	8.9 ± 5.1
Tetramethylammonium	3.0 ± 0.5	1.5 ± 0.6	240 ± 110
DMPP	0.19 ± 0.04	0.50 ± 0.13	5.6 ± 1.8
Carbamylcholine	2.0 ± 0.3	7.0 ± 1.4	6.2 ± 2.9
β-Methylcarbamylcholine	>1000	>1000	47 ± 19
Oxotremorine	260 ± 110	800 ± 400	0.16 ± 0.04
Atropine	770 ± 220	250 ± 110	0.0028 ± 0.0021
Hexamethonium	450 ± 190	>1000	260 ± 50
Pentolinium	260 ± 80	>1000	93 ± 34
d-Tubocurarine	32 ± 8	1.3 ± 0.4	10 ± 4
Decamethonium	21 ± 2	22 ± 7	13 ± 1
Gallamine	95 ± 16	70 ± 22	7.6 ± 2.6
Tetraethylammonium	73 ± 17	30 ± 8	150 ± 20
Mecamylamine	>1000	>1000	120 ± 30
α-BTX	>1	0.00072 ± 0.00026	>1

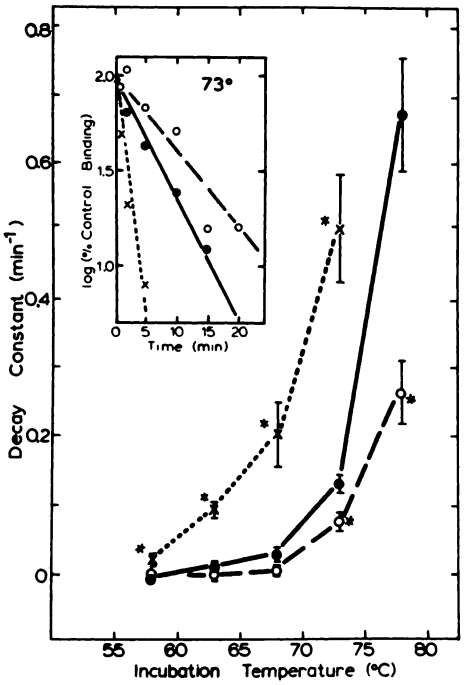

FIG. 9. *Thermal sensitivity of [^{3}H]nicotine, [^{125}I]α-BTX, and [^{3}H]QNB binding*

Whole-brain particulate protein was incubated for varying amounts of time (1–30 min) at the temperatures indicated. Standard binding assays were conducted at 37° for nicotine (●), BTX (○), and QNB (×). Binding at each time point was determined, and log(% control binding) was graphed as a function of time at elevated temperature as shown in the *inset* for an incubation temperature of 73°. Slopes (± standard deviation) were determined by regression analysis for each ligand at each temperature. Decay constants (2.303 × slope) were calculated and graphed as a function of incubation temperature. *Asterisks* denote decay constants significantly different ($p < 0.05$) from those for nicotine binding.

Thermal sensitivity of binding sites. The effect of incubation of the brain protein at elevated temperatures was investigated to provide a further comparison of the three ligand binding sites. In the *inset* to Fig. 9 the time courses for the disappearance of [^{3}H]nicotine, [^{125}I]α-BTX, and [^{3}H]QNB binding are presented. The plots of log(% control binding) versus time were linear for all three ligands. Similar plots constructed for other temperatures were comparable to that shown. When the decay constants for binding of all three ligands were calculated from the slopes of the lines at five elevated temperatures, the constants increased as the incubation temperature was raised. This increase in the decay constant was observed for the binding of all three ligands. The thermal lability of the binding sites for the three ligands differed markedly from each other. The [^{3}H]QNB binding site was most sensitive. Although the curves for the nicotine and α-BTX binding sites were similar to each other, the nicotine binding site was more sensitive

to thermal degradation than was the α-BTX binding site. Comparison of the decay constants by comparison of the slopes of the lines from data similar to those shown in the *inset* to Fig. 9 revealed that these values differed significantly ($p < 0.05$) at 73° and 78°.

DISCUSSION

The binding of [^{3}H]nicotine to brain tissue appears to be a temperature-dependent, reversible, saturable process. Scatchard analysis indicates that at 20° and 37° binding occurs at what appears to be a single site, whereas at 4° evidence for a second, low-affinity site was obtained. The whole-brain K_D for the high-affinity site was 59 nM, and maximal binding was 88 fmoles/mg of protein. This binding was unevenly distributed in brain, with relatively high concentrations in striatum and midbrain and very low concentrations in cerebellum. Binding of nicotine was inhibited by micromolar (or lower) concentrations of a number of classical nicotinic agonists, but classical nicotinic antagonists were weak inhibitors of binding. Muscarinic agonists and antagonists also proved to be weak inhibitors.

Several recent studies have demonstrated the existence of saturable, high-affinity [^{3}H]nicotine binding to brain (15–18). The results obtained in the current study agree closely with those of Romano and Goldstein (17), who used whole rat brain membranes. They reported a K_D for nicotine of 43 nM, a value comparable to that of 59 nM detected in our studies. The B_{max} value of 4.4 fmoles/mg of tissue [multiply by 15–20 mg of tissue (wet weight) per milligram of particulate protein for comparison] is similar to our value of 88 fmoles/mg of protein. Abood *et al.* (16), also using rat brain membranes, found a K_D of 5.6 nM for nicotine. This low K_D is not fully consistent with the IC_{50} value of 120 nM for L-nicotine reported by these investigators. When the apparent K_I for L-nicotine is calculated from the IC_{50} value using the equation of Cheng and Prusoff (21) [$IC_{50} = K_I(1 + S/K_M)$], a value of 26 nM is obtained. This value was inserted into the equation as a new estimate of K_D, and a new estimate of the K_I value was then calculated. This process was repeated until no further change in either K_I or K_D occurred. The K_I values obtained from this calculation are 110 nM (when binding is assumed to be stereospecific) and 100 nM (when it is assumed to be nonstereospecific). The corresponding K_D values were 220 nM and 100 nM. The basis for this inconsistency between K_D and K_I is not readily apparent. Sershen *et al.* (18) reported a K_D of 100–400 nM and a corresponding B_{max} of 160 fmoles/mg of protein. The studies on nicotine binding published to date show general agreement inasmuch as the B_{max} values are approximately 100 fmoles/mg of protein and the K_D values are in the range of 6–400 nM.

The effect of potential competitive inhibitors on [^{3}H]nicotine binding has been investigated by several groups. Romano and Goldstein (17) tested many potential competitive inhibitors, including nicotinic and muscarinic agonists and antagonists as well as noncholinergic agents. The nicotinic agonists (ganglionic stimulants) were the most potent inhibitors. Our results agree both qualitatively and quantitatively with theirs. Abood *et al.* (16) tested fewer compounds, and they observed inhibition of nicotine binding by the cholinergic agonists nicotine and carbamylcholine. Carbamylcholine was approximately two orders of magnitude less potent in inhibiting the nicotine binding than was L-nicotine, an observation which agrees with our observations and those of Romano and Goldstein (17). Although Sershen *et al.* (18) observed inhibition of nicotine binding by L-nicotine, they failed to obtain inhibition by acetylcholine. These authors did not indicate whether a cholinesterase inhibitor was added to their incubation media. In the absence of enzyme inhibition, little intact acetylcholine would remain in the incubation medium and, consequently, little inhibition would be expected. Our data obtained with tissue treated with DFP to inhibit acetylcholinesterase activity indicate that acetylcholine is a potent inhibitor of nicotine binding. The results of the present study are in agreement with those of both Romano and Goldstein (17) and Abood *et al.* (16) which show that nicotine binding is inhibited by L-nicotine and nicotinic, cholinergic agonists.

There is some disagreement on whether [^{3}H]nicotine binding is stereospecific. Romano and Goldstein (17) found that L-nicotine was approximately 50-fold more potent than D-nicotine in inhibiting [^{3}H]nicotine binding. Likewise, Abood *et al.* (16) found the L-isomer to be 30-fold more potent than the D-isomer. Similarly, we observed that the L-isomer is 30- to 40-fold more potent than is the D-isomer. However, Sershen *et al.* (18) found no sterospecificity. There are several problems with the latter study. These investigators observed two components of nicotine binding with widely different K_D and B_{max} values. When their binding constants are used to calculate binding to the high- and low-affinity sites, about 55% of the counts are bound to the high-affinity sites and the remaining 45% to low-affinity sites. Therefore, the effects of inhibitors were determined on both nicotine binding sites. Since the dose-response curves were not extended below 1 μM added inhibitor, at which concentration 30% of the counts had been displaced by L-nicotine and 20% by D-nicotine, it is difficult to estimate an IC_{50} for either compound at the high-affinity site. Examination of the data reveals that L-nicotine was more potent than D-nicotine in inhibiting [^{3}H]nicotine binding at low concentrations of added inhibitor; i.e., the high-affinity site is stereospecific. The racemic mixture of [^{3}H]nicotine was used in all of these studies. Since there is a 30- to 40-fold difference in the K_I values for the stereoisomers, it seems probable that binding at the high-affinity site is almost exclusively that of the L-isomer. However, little stereospecificity was seen at the low-affinity site which was detected at 4°. Therefore, both stereoisomers bind at this site.

Classical nicotinic antagonists, in contrast to agonists, are very poor inhibitors of [^{3}H]nicotine binding. The relative ineffectiveness of these compounds has been observed by Romano and Goldstein (17), by Abood *et al.* (16), by Sershen *et al.* (18), and in the present study. This ineffectiveness, coupled with the observation that nicotinic antagonists did not block nicotine-induced prostration, led Abood *et al.* (22) to suggest that nicotine binds to a noncholinergic site in rat brain. However, the prostration syndrome is blocked by *N*-alkyl piperidine and *N*-alkyl nornicotine, which are also inhibitors of nicotine binding (22). Sershen *et al.* (18) have also argued that nicotine binding occurs at a noncholinergic site.

Other possible explanations for the relative inability of nicotinic antagonists to block nicotine binding include the suggestion by Romano and Goldstein that an agonist-induced shift of the receptor to a high-affinity, agonist-selective state may occur during the incubation period. A shift of this sort has been reported for α-BTX binding to rat brain when membranes are incubated with cholinergic agonists (23). Such a shift might explain the relative inability of antagonists to block nicotine binding, as well as explain a K_D value which is substantially lower than the concentration of the drug required to elicit a pharmacological response. Another plausible explanation is that the antagonists may not bind to the same site as does nicotine. Ascher *et al.* (24) have observed that classical nicotinic antagonists such as *d*-tubocurarine, hexamethonium, and decamethonium block transmission in the parasympathetic neurons of the submandibular ganglion of the rat more effectively in the presence of agonists. As agonist concentration increases, blockade by the antagonists increases. These investigators suggest that the antagonists bind to the open form of the channel-receptor complex while agonists bind to the closed form. Clearly, a better understanding of the nicotine binding site will be required to explain fully the ineffectiveness of classical nicotinic antagonists in inhibiting nicotine binding and the nicotine-induced prostration syndrome (22).

The studies by Romano and Goldstein (17) and Sershen *et al.* (18) noted that nicotine binding has two components: high-affinity sites and low-affinity sites. Sershen *et al.* (18) obtained K_D values of 100 nM and 20 μM for the high- and low-affinity sites, respectively. The K_D values obtained by Romano and Goldstein (17) for these two sites were lower (i.e., 28 nM and 460 nM in one experiment). These two groups used different buffers and different incubation temperatures; our results indicate that neither temperature nor 100 mM Tris has an effect on the kinetic properties of the high-affinity binding site. The quantitative differences in the K_D values for the high-affinity site are relatively small (less than one order of magnitude) and may represent small methodological or species differences. Although nanomolar K_D values have been found by all investigators to date (refs. 15–18; present study), the low-affinity site has not been uniformly detected. It seems to us that detection of this site is temperature-dependent. Romano and Goldstein (17) carried out their incubations at 37°, but their samples were chilled on ice for 20 min before dilution with 4 ml of cold buffer and filtering. We did not detect the low-affinity binding site when incubations were carried out in the same buffer at 20° or at 37°, but it was detected at 4°. It seems unlikely that an interconversion between low- and high-affinity sites occurs with change in temperature, since the number of high-affinity sites (B_{max}) does not vary with incubation temperature. Since neither atropine nor oxotremorine inhibits the binding of nicotine to the low-affinity site (data not shown), it is not likely that the low-affinity binding is occurring at the mAChR. Finally, very little variance was observed among the different brain regions with regard to the amount of low affinity binding (data not shown). Therefore, it seems possible that some effect of temperature on the membrane is responsible for the appearance of the low-affinity nicotine binding.

Our data are consistent with the argument that nicotine binds to a cholinergic site. This prompted the series of experiments which compared nicotine binding with the binding of QNB and α-BTX. We found that the muscarinic receptor, as measured by QNB binding, occurs in approximately 20 times greater concentration in whole mouse brain than does nicotine binding and is nearly 100 times greater than α-BTX binding. These results for QNB binding and α-BTX binding are in reasonable agreement with those of others (1, 9, 13, 14, 23, 25). Salvaterra and Foders (9) studied QNB and α-BTX binding in a number of species. These investigators reported similar amounts of both QNB and α-BTX binding in whole brain of rats (Sprague-Dawley) and mice (Swiss). They noted that QNB binding in Swiss mice is approximately 50 times greater than is α-BTX binding. Differences in α-BTX binding among mouse strains were also observed. Similarly, Aronstam *et al.* (25) and Marks *et al.* (26) have reported strain differences in QNB binding. Thus, the 2-fold difference between the ratio of QNB/α-BTX binding seen in our study and that of Salvaterra and Foders (9) is not surprising. Clearly, QNB binding is found in much greater concentration than is α-BTX binding.

Nicotine binding and α-BTX binding have not been directly compared previously. We observed a 4-fold difference in binding between the two ligands, and found that nicotine inhibits α-BTX binding with an apparent K_I value of 0.81 μM. Other studies have also reported a micromolar IC_{50} or K_I value for the inhibition of α-BTX binding by nicotine (12–14). Since this inhibition occurs at concentrations which are relevant to the physiological effects of nicotine, these data may indicate that nicotine exerts some of its actions at the α-BTX site. However, since α-BTX fails to inhibit nicotine binding and since regional distributions in brain are different, it is unlikely that the α-BTX binding site has four nicotine binding sites associated with it. Patrick and Stallcup (27) have presented immunological evidence that the nicotinic receptor in sympathetic ganglia and the α-BTX binding component are physically distinct entities. Perhaps nicotine binds to this receptor which is found in association with the α-BTX binding component.

Another major distinction between the three ligands is found in the inhibition pattern. The observation that atropine and oxotremorine are ineffective in blocking nicotine binding makes it unlikely that nicotine is binding to some super-high affinity muscarinic receptor. For both nicotine and α-BTX, nicotinic agonists are much more potent inhibitors of binding than are antagonists. This has been demonstrated previously for α-BTX (11). Careful inspection of the data in Table 3 reveals that lobeline and nicotine are much more effective in inhibiting nicotine binding than they are in inhibiting α-BTX binding. Antagonists do not differentiate nicotine and α-BTX binding. Thus, the inhibitor studies provide compelling evidence to differentiate nicotine binding from QNB binding, but only suggestive data that differentiate between nicotine and α-BTX binding.

The regional distribution study also provides data suggesting that nicotine binding is not associated with the QNB or α-BTX binding sites. Our regional analyses of QNB binding and α-BTX binding agree reasonably well

with those of others (9). The patterns of regional distribution of the binding of the three ligands in mouse brain regions differ markedly from each other (Table 2); the finding that these three ligands seem to be, for the most part, distributing independently of one another adds to the argument that they are binding to different cholinergic receptors.

Perhaps the most compelling data which differentiate the nicotine and α-BTX binding sites were obtained in the thermal denaturation study. Saitoh *et al.* (28) have presented evidence that heat inactivation studies can detect subtle differences in the environment or physical state of the α-BTX binding site. Our heat inactivation study demonstrated that the QNB binding site is much more labile than are the nicotine and α-BTX sites. The two nicotinic sites were less thermolabile and were clearly differentiated only at the higher incubation temperatures (73° and 78°). Taken together, the drug inhibition and thermal denaturation studies suggest that the nicotine and α-BTX binding sites are separate entities, but that they are similar.

In conclusion, the results of the present study confirm the presence in brain of a saturable, reversible nicotine binding site. This site is clearly not the same site as the one which binds QNB; i.e., it is not muscarinic. Although it shares some similarities with the α-BTX site, differences in regional distribution, in inhibitor sensitivity, and in thermal stability suggest that the nicotine and α-BTX sites are different. In view of the apparent affinity of nicotine for both sites, it seems reasonable to speculate that the behavioral effects of nicotine may be mediated via an effect at both binding sites.

ACKNOWLEDGMENTS

The authors wish to thank Dr. Nancy Zahniser, Department of Pharmacology, University of Colorado Health Sciences Center, for helpful discussions concerning the preparation of this paper; Mrs. Rebecca Miles for expert editorial assistance; and Ms. Barbi Kirwin for typing the manuscript. We are also grateful to Dr. Yukiteru Obi, of the Japan Tobacco and Salt Public Corporation (Yokohama, Japan), for supplying us with D-(+)-nicotine.

REFERENCES

1. Yamamura, H. I., and S. H. Snyder. Muscarinic cholinergic binding in rat brain. *Proc. Natl. Acad. Sci. U. S. A.* **71**:1725–1729 (1974).
2. Oswald, R. E., and J. A. Freeman. Alpha-bungarotoxin binding and central nervous system nicotinic acetylcholine receptors. *Neuroscience* **6**:1–14 (1981).
3. Morley, B. J., G. E. Kemp, and P. Salvatera. α-Bungarotoxin binding sites in the CNS. *Life Sci.* **24**:859–872 (1979).
4. Chou, T. C., and C. Y. Lee. Effect of whole and fractionated cobra venom on sympathetic ganglion transmission. *Eur. J. Pharmacol.* **8**:326–330 (1969).
5. Carbonetto, S. T., D. M. Fambrough, and K. J. Muller. Nonequivalence of α-bungarotoxin receptors and acetylcholine receptors in chick sympathetic neurons. *Proc. Natl. Acad. Sci. U. S. A.* **75**:1016–1020 (1978).
6. Ko, C. P., H. Burton, and R. P. Bunge. Synaptic transmission between rat spinal cord explants and dissociated cervical ganglion neurons in tissue culture. *Brain Res.* **117**:437–460 (1976).
7. Miledi, R., and A. C. Szczepaniak. Effect of *Dendroaspis* neurotoxins on synaptic transmission in the spinal cord of the frog. *Proc. R. Soc. Lond. B Biol. Sci.* **190**:267–274 (1975).
8. Duggan, A. W., J. G. Hall, and C. Y. Lee. Alpha-bungarotoxin, cobra neurotoxin and excitation of Renshaw cells by acetylcholine. *Brain Res.* **107**:166–170 (1976).
9. Salvaterra, P. M., and R. E. Foders. [^{125}I]$_2$ α-Bungarotoxin and [^{3}H]quinuclidinylbenzilate binding in central nervous systems of different species. *J. Neurochem.* **32**:1509–1517 (1979).
10. Salvaterra, P. M., and H. R. Mahler. Nicotinic acetylcholine receptor from rat brain: solubilization, partial purification, and characterization. *J. Biol. Chem.* **251**:6327–6334 (1976).
11. McQuarrie, C., P. M. Salvaterra, A. DeBlas, J. Routes, and H. R. Mahler. Studies on nicotinic acetylcholine receptors in mammalian brains: preliminary characterization of membrane-bound α-bungarotoxin receptors in rat cerebral cortex. *J. Biol. Chem.* **251**:6335–6339 (1976).
12. Schmidt, J. Drug binding properties of an α-bungarotoxin-binding component from rat brain. *Mol. Pharmacol.* **13**:283–290 (1977).
13. Moore, W. M., and R. N. Brady. Studies of nicotinic acetylcholine receptor protein from rat brain. II. Partial purification. *Biochim. Biophys. Acta* **498**:331–340 (1977).
14. Morley, B. J., J. F. Lorden, G. B. Brown, G. E. Kemp, and R. J. Bradley. Regional distribution of nicotinic acetylcholine receptor in rat brain. *Brain Res.* **134**:161–166 (1977).
15. Schleifer, L. S., and M. E. Eldefrawi. Identification of the nicotinic and muscarinic acetylcholine receptors in subcellular fractions of mouse brain. *Neuropharmacology* **13**:53–63 (1974).
16. Abood, L. G., D. T. Reynolds, and J. M. Bidlack. Stereospecific ^{3}H-nicotine binding to intact and solubilized rat brain membranes and evidence for its noncholinergic nature. *Life Sci.* **27**:1307–1314 (1980).
17. Romano, C., and A. Goldstein. Stereospecific nicotine receptors on rat brain membranes. *Science (Wash. D. C.)* **210**:647–650 (1980).
18. Sershen, H., M. E. A. Reith, A. Lajtha, and J. Gennaro, Jr. Noncholinergic, saturable binding of (±)-[^{3}H]nicotine to mouse brain. *J. Receptor Res.* **2**:1–15 (1981).
19. Lowry, O. H., N. H. Rosebrough, A. C. Farr, and R. J. Randall. Protein measurement with Folin phenol reagent. *J. Biol. Chem.* **193**:265–275 (1951).
20. Molinoff, P. B., B. B. Wolfe, and G. A. Weiland. Quantitative analysis of drug-receptor interactions. II. Determination of the properties of receptor subtypes. *Life Sci.* **29**:427–444 (1981).
21. Cheng, Y.-C., and W. H. Prusoff. Relationship between the inhibition constant (K_i) and the concentration of inhibitor which causes 50 percent inhibition (I_{50}) of an enzymatic reaction. *Biochem. Pharmacol.* **22**:3099–3108 (1973).
22. Abood, L. G., K. Lowy, A. Tometska, and M. MacNeil. Evidence for a noncholinergic site for nicotine's action in brain: psychopharmacological, electrophysiological and receptor binding studies. *Arch. Int. Pharmacodyn. Ther.* **237**:213–229 (1979).
23. Lukasiewicz, R. J., and E. L. Bennett. α-Bungarotoxin binding properties of a central nervous system nicotinic receptor. *Biochim. Biophys. Acta* **544**:294–308 (1978).
24. Ascher, P., W. A. Lange, and H. P. Rany. Studies on the mechanism of action of acetylcholine antagonists on rat parasympathetic ganglion cells. *J. Physiol. (Lond.)* **295**:139–170 (1979).
25. Aronstam, R. S., C. Kellogg, and L. G. Abood. Development of muscarinic cholinergic receptors in inbred strains of mice: identification of receptor heterogeneity and relation to audiogenic seizure susceptibility. *Brain Res.* **162**:231–241 (1979).
26. Marks, M. J., D. M. Patinkin, L. D. Artman, J. B. Burch, and A. C. Collins. Genetic influences on cholinergic drug response. *Pharmacol. Biochem. Behav.* **15**:271–279 (1981).
27. Patrick, J., and W. B. Stallcup. Immunological distinction between acetylcholine receptor and the α-bungarotoxin-binding component on sympathetic neurons. *Proc. Natl. Acad. Sci. U. S. A.* **74**:4689–4692 (1977).
28. Saitoh, T., L. P. Wennogle, and J.-P. Changeux. Factors regulating the susceptibility of the acetylcholine receptor protein to heat inactivation. *F. E. B. S. Lett.* **108**:489–494 (1979).

Send reprint requests to: Dr. Allan C. Collins, Institute for Behavioral Genetics, Box 447, University of Colorado, Boulder, Colo. 80309.